THE ASTROPHYSICAL JOURNAL, 417:287–297, 1993 November 1

ABUNDANCES IN CH SUBGIANTS: EVIDENCE OF MASS TRANSFER ONTO MAIN-SEQUENCE COMPANIONS

VERNE V. SMITH,[1] HOWARD COLEMAN,[2] AND DAVID L. LAMBERT[3]
Department of Astronomy and McDonald Observatory, The University of Texas at Austin, Austin, TX 78712
Received 1993 March 2; accepted 1993 April 12

ABSTRACT

Carbon, oxygen, and *s*-process abundances, as well as abundances of other metals, such as iron, calcium, or nickel, are presented for a sample of nine CH subgiants. The abundances are derived from high-resolution, high–S/N spectra. The CH subgiants in this sample are found to have mild metal-deficiencies ([Fe/H] $\approx$ 0.0 to -0.4), a range of *s*-process overabundances ([*s*-process/Fe] $\approx {}^{+}0.2$ to ${}^{+}1.0$), and C/O ratios from 0.4 to 2.0. When compared to the barium giant stars, the CH subgiants tend to have larger C/O ratios, however, the barium giants have deep convective envelopes that are presumably absent from the CH subgiants, which lie on, or near, the main sequence. As the CH subgiants evolve up the red giant branch and develop deep convective envelopes, their carbon-rich atmospheres will be mixed with material less abundant in C and their C/O ratios will decrease. It is thus quite probable that the majority of the barium giant stars have evolved from CH subgiant progenitors. The heavy-element abundance distributions of the CH subgiants studied here, as well as published analyses of other barium and CH giant stars, indicate that the *s*-process abundance enhancements are created by neutrons from the $^{13}C(\alpha, n)^{16}O$ neutron source.

Subject headings: binaries: close — stars: abundances — stars: giant

1. INTRODUCTION

The subgiant CH stars are a puzzling group of chemically peculiar stars sharing many of the abundance peculiarities observed in the giant barium and CH stars, yet have modest luminosities typical of dwarfs and subgiants. These stars were first isolated as a group by Bond (1974), who noted them to be, typically, G-dwarf and subgiant stars with $M_v \sim +2$ to $+4$ and anomalously strong heavy-element ($Z > 30$) lines compared to the Fe-peak lines.

High-resolution abundance analyses were first carried out by Sneden & Bond (1976) and Luck & Bond (1982; hereafter LB82) who confirmed the low luminosities (through high surface gravities) and heavy-element overabundances in these stars. These studies found that, as a group, the subgiant CH stars exhibit mild abundance deficiencies of most of the "metals" ([Fe/H] ~ -0.2 to -0.5, in the standard notation where $[X] = \log X - \log X_{\odot}$) with rather large enhancements of the heavy *s*-process elements ([*s*-process/Fe] $\sim +0.3$ to $+1.0$): such *s*-process overabundances are typical of the more luminous barium and CH giant stars. In addition to the substantial *s*-process enhancements, LB82 found large carbon overabundances ([C/Fe] $\sim +0.4$ to $+1.2$) from an analysis of permitted C I lines. More recent abundance analyses have been carried out for carbon and oxygen by Sneden (1983) and for the heavy *s*-process elements by Krishnaswamy & Sneden (1985). Sneden (1983) based his carbon analysis on molecular lines (CH and C_2), while using the [O I] line to derive O abundances; he derives slightly lower C abundances for four stars in common with LB82: Sneden derives an average C abundance that is 0.3 dex lower than LB82. For three stars for which he has both C and O abundances, Sneden (1983) derives C/O ratios of 0.6, 0.8, and 1.0, and these are larger than the solar value of C/O = 0.48 (Anders & Grevesse 1989; Grevesse et al. 1991). LB82 obtain somewhat larger C/O ratios which range from 0.6 to 1.6, with an average C/O = 1.2 for six stars.

Krishnaswamy & Sneden (1985) studied the heavy-element *s*-process abundance pattern in two CH subgiants and found the *s*-process abundance distribution to be characterized by an exponential neutron exposures with $\tau_0 \approx 0.2$ mb^{-1}. This is somewhat less than that derived for most barium stars, with Smith (1984) finding typical values of $\tau_0 \sim 0.3$–0.4 mb^{-1} for seven stars, while Tomkin & Lambert (1983, 1986) find $\tau_0 \sim 0.6$ mb^{-1} for three barium and mild barium stars; whether there is a significant difference in the neutron exposures found in the CH subgiants with respect to the barium remains to be seen. In a recent abundance analysis of CH subgiants, and a review of abundances in the barium giants, Luck and Bond (1991–LB91) conclude that the *s*-process abundance distributions are similar, within the uncertainties, for the CH subgiants and the barium stars and that the CH subgiants will evolve into the barium giant stars.

If Luck & Bond (1991) are correct, then the origin of the abundance peculiarities in the CH subgiants is the same as that of the barium and CH giant stars: the mass transfer of ^{12}C-rich and *s*-process rich material from an evolved companion that was a thermally pulsing (TP) asymptotic giant branch (AGB) star onto the star that we now observe to be a barium or CH giant star or a CH subgiant. The foundation for this picture of the origin of these low-luminosity peculiar giants is the radial-velocity observations of McClure and collaborators (McClure, Fletcher, & Nemec 1980; McClure 1983, 1984, 1989; McClure & Woodsworth 1990) who have demonstrated that the barium stars, as well as the CH giants and subgiants, are most probably all single-line spectroscopic binaries with unseen (in most cases) companions that are probably white dwarfs: the demonstrated incidence of binary systems among these peculiar stars is 90% for the barium stars, 92% for the CH giants, and 70% for the CH subgiants.

In the case of the barium and CH giants, the approximately 10% of the stars that are apparently single may be plausibly

[1] E-mail address: verne@astro.as.utexas.edu.
[2] E-mail address: howard@astro.as.utexas.edu.
[3] E-mail address: dll@astro.as.utexas.edu.

attributed to systems with long periods and/or high inclined orbital planes such that the radial-velocity variations are extremely small, i.e., the hypothesis that *all* barium and CH giants belong to binary systems is readily defensible. At present, the CH subgiants present a distinctly lower fraction of spectroscopic binaries. Since this fraction is markedly greater than the fraction reported for normal giants and subgiants of 15%–20% (Harris & McClure 1983), it is presumed that CH subgiants are predominantly and probably exclusively members of binary systems. Perhaps, the lower reported frequency of spectroscopic binaries is due to contamination of the sample with normal stars.

Since it is supposed that all CH subgiants (including the main-sequence F dwarfs with *s*-process enhancements), barium, and CH giants belong to long-period spectroscopic binary systems, it is natural to suppose that the majority of these stars belong to the evolutionary sequence of barium dwarf to CH subgiant to barium, or CH giant. It is possible that, following mass transfer from the AGB star (now the white-dwarf companion), the barium star created from the initially less massive star was not at the beginning of the evolutionary sequence outlined above. However, one expects the bypassing of the barium dwarf stage to occur infrequently as direct production of a barium giant requires the initial mass ratio to be very nearly unity. In short, the natural hypothesis supposes barium dwarfs to evolve through a subgiant phase and then into barium giants. If this hypothesis is true, these classes of peculiar stars must show considerable similarity of composition. Differences arising from the first dredge-up experienced in the evolution of a subgiant to a giant are expected and are predictable in a qualitative sense.

The purpose of this study is to determine carbon and oxygen abundances in a sample of CH subgiants to see if the rather large C abundances obtained by LB82 are typical of these stars and to compare these abundances in the CH subgiants to the barium giants as a test of the hypothesis that the former evolve into the latter. In addition, we obtained data for a small sample of *s*-process lines to investigate if there is a relation between the carbon abundances and the *s*-process overabundances as is found for the barium stars (Lambert 1985) or the MS and S stars (Smith & Lambert 1990).

2. OBSERVATIONS AND ANALYSIS

Spectra were obtained for nine CH subgiants; these particular stars were chosen to be primarily those studied by LB82, Sneden (1983), Krishnaswamy & Sneden (1985), and Smith & Lambert (1986): the program stars are listed in Table 1. Included in Table 1 are the model atmosphere parameters used for this sample of stars: listed are the effective temperature, surface gravity, microturbulent velocity, and overall metallicity for each model. As most of these stars have been studied in detail by the above mentioned studies, we adopt their values for $T_{\rm eff}$, log g, and [M/H]. Effective temperatures from these previous studies were determined from broad-band colors or spectroscopic analyses and we can make no improvement on those determinations here. Surface gravities were fixed by demanding that Fe I and Fe II lines yield the same abundance (see below), and we checked the surface gravities derived by these previous studies from our own Fe I/Fe II analysis.

As the CH subgiants are not vastly different from the Sun in $T_{\rm eff}$ and log g, we generated scaled solar models from the Holweger & Müller (1974) solar atmosphere for the particular $T_{\rm eff}$ – log g – [M/H] combination. Again, the metallicity for these models was taken from the previous determinations and, in every case, our derived overall metallicities were close enough to the model metallicities (differences of $\lesssim$0.2 dex) to justify no further iterations on the model metallicities. One star has not been studied before at high resolution, HD 219116, and an estimate of its atmospheric parameters was obtained by noting that its spectrum is very similar to HD 125079, so we used the model from this star for HD 219116 and found it to yield satisfactory results.

The ultimate key to an abundance analysis are the spectra and their absorption lines and we obtained a series of spectra with the McDonald Observatory's 2.7 m telescope, coudé spectrometer, and a TI 800 × 800 pixel CCD. Typical scale factors for these spectra were about 0.06 Å pixel^{-1} (with 15 μm pixels) with three-pixel resolution. Each spectrum contained approximately 50 Å of spectra, and we obtained spectra for six regions centered on the following wavelengths: 5120 Å, 5360 Å, 6158 Å, 6420 Å, 7115 Å, and 7765 Å. These wavelength regions provided a variety of elemental lines including C I, O I, a selection of Fe I and Fe II lines, and a sample of the heavier *s*-process species, such as Y I, Y II, Zr I, Zr II, Ba II, and Nd II. Spectra were reduced with the IRAF software package and equivalent widths were measured as input data for the abundance analysis. Sample spectra are shown in Figures 1, 2, and 3 for the star HD 216219. Figure 1 shows the C I lines near 7115 Å that were used for the C abundances: the bottom spectrum, shifted by 0.5 in the relative intensity scale, of 4 Tau, a rapidly rotating (v sin i = 261 km s^{-1}) A0 V star (Hoffleit & Jaschek 1982) illustrates the few weak telluric H_2O lines which contaminate this region. The O I triplet is illustrated in Figure 2, again with a rapidly rotating hot star (ξ Aql, A0 V, v sin i = 331 km s^{-1}; Hoffleit & Jaschek 1982) to illustrate the lack of telluric contamination in this region. Finally, Figure 3 shows

TABLE 1

PROGRAM STARS AND ATMOSPHERIC PARAMETERS

Star	$T_{\rm eff}$ (K)	log g (cm s^{-2})	ξ (km s^{-1})	[M/H]	Source[a]
HD 4395	5450	3.3	1.3	−0.3	S
HD 11377	6000	4.1	1.2	−0.2	LB
HD 88446	6000	4.5	0.9	−0.4	LB
HD 89948	5950	4.1	0.8	−0.5	S
HD 125079	5300	3.5	1.4	−0.3	SL
HD 182274	6000	4.5	0.6	−0.4	LB
HD 204613	5650	3.8	0.9	−0.5	S
HD 216219	5600	3.2	1.6	−0.3	S
HD 219116	5300	3.5	2.0	−0.3	This study

[a] LB = Luck & Bond 1982; S = Sneden 1983; SL = Smith & Lambert 1986.

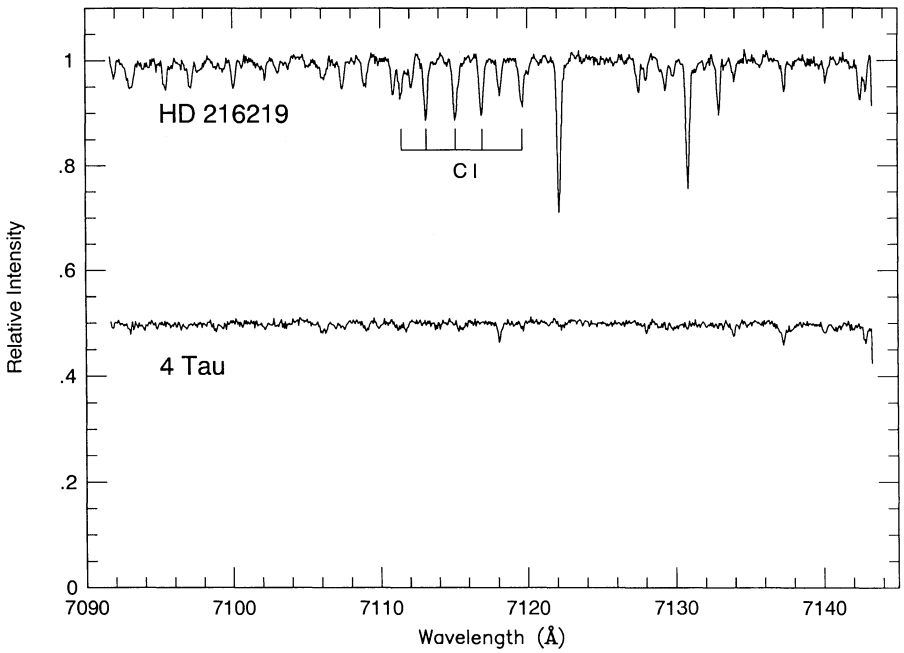

FIG. 1.—Sample spectra of the C I lines near 7115 Å in the CH subgiant HD 216219. The bottom spectrum is a rapidly rotating ($v \sin i = 261$ km s^{-1}) star which illustrates weak telluric H_2O lines in this region: this spectrum has been shifted down by 0.5 in relative intensity.

an expanded view of the region near 6150 Å to show some of the *s*-process heavy-element lines. The list of lines used in the abundance analysis, arranged by element, as well as measured equivalent widths, are presented in Table 2. We determined abundances in the CH subgiants relative to the Sun, so most of the *gf*-values listed in Table 2 are "solar *gf*-values"; these *gf*-values were derived from measuring equivalent widths from the solar atlas of Debouille, Neven, & Roland (1973) and using the empirical solar atmosphere from Holweger and Müller (1974), with a global microturbulence of $\xi = 0.8$ km s^{-1}, and solar abundances from Anders & Grevesse (1989). The analysis of LB82 used the same approach; thus our abundances can be compared directly to theirs with only minor differences.

We used the same C I and O I lines (and *gf*-values) used by LB82 to determine C and O abundances: again, our abundances can then be compared directly to LB82. The C I *gf*-values in LB82 were derived from the Sun, while the O I oscillator strengths are from Wiese, Glennon, & Smith (1966):

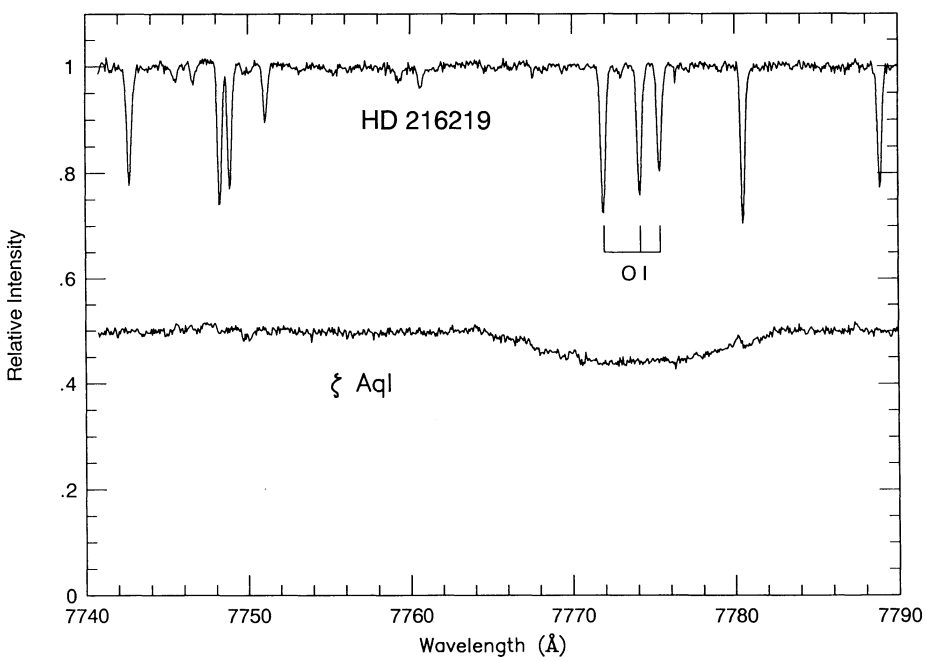

FIG. 2.—Sample spectra showing the O I triplet in HD 216219 and the same region in a rapidly rotating ($v \sin i = 331$ km s^{-1}) star (where the spectrum is shifted in intensity) to show that the O I lines are free from telluric contamination.

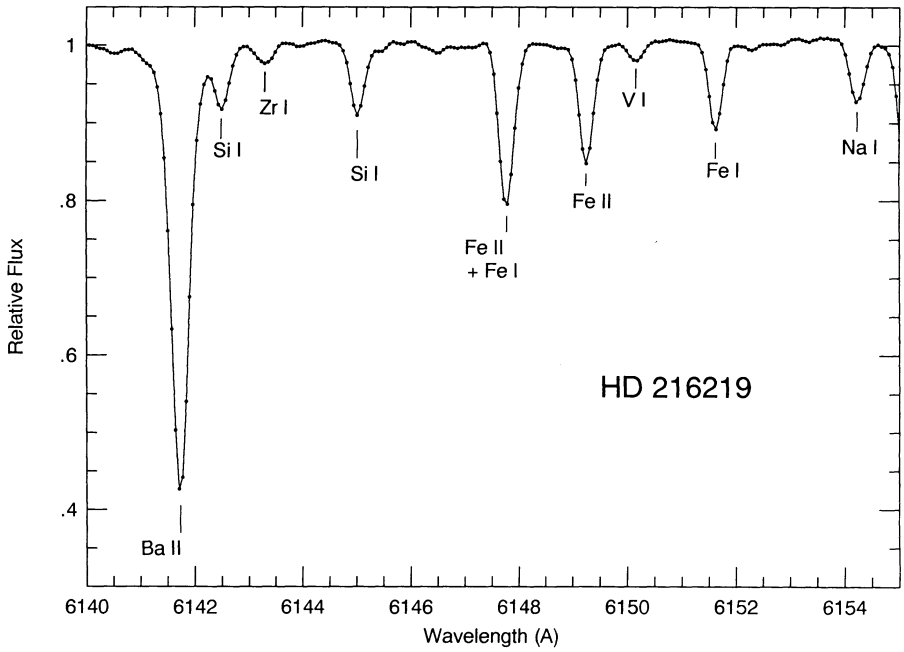

FIG. 3.—An expanded view of the spectral region near 6150 Å in the CH subgiant HD 216219. This figure illustrates some of the Fe and heavy-element lines used in the abundance analysis.

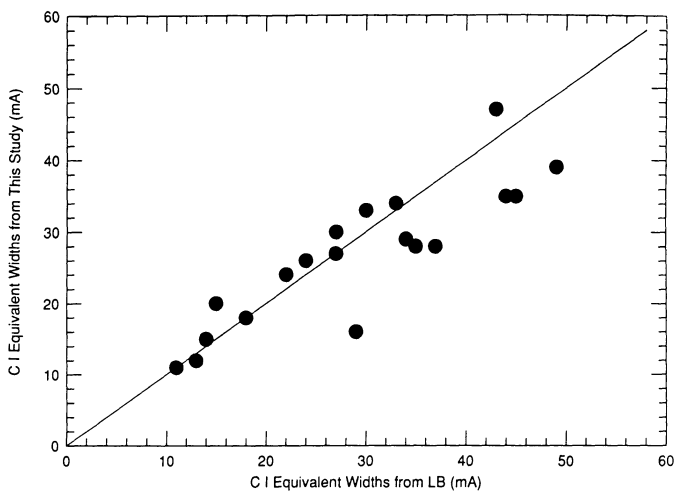

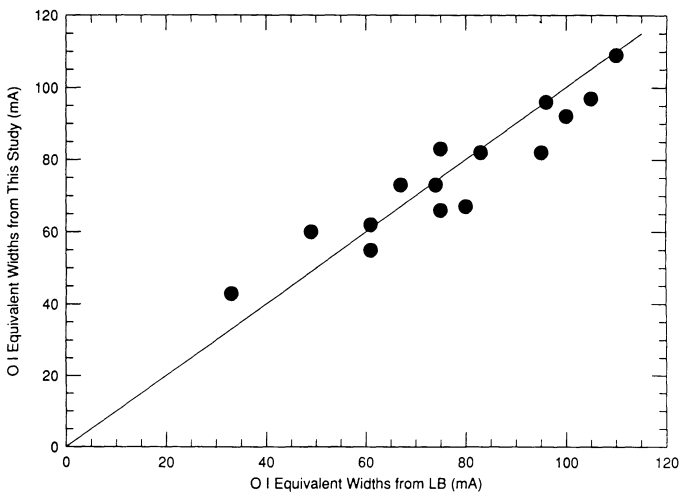

these O I *gf*-values are only 0.02 dex smaller than the more recent values used by Tomkin et al. (1992). We compare equivalent widths which our two studies have in common in Figure 4. In the top panel of Figure 4, we compare the C I equivalent widths: these data represent various measurements of the five lines near 7115 Å for stars that we have in common with LB82. Overall, the agreement is good (the solid line represents perfect agreement): for equivalent widths less than 30 mÅ, the differences are typically less than 3 mÅ. Above line strengths of about 30 mÅ, LB82 tend to obtain somewhat larger equivalent widths by about 5–10 mÅ. The source of this offset is unknown, however, our two studies used different detectors. A comparison of the O I 7770 Å triplet lines are shown in the bottom panel of Figure 4. These lines are generally much stronger than the C I lines and the agreement between our measurements and those of LB82 are good (the solid line again represents perfect agreement): the equivalent widths agree to within 10 mÅ. Abundances are derived from the equivalent widths and model atmospheres using the most recent version of the LTE synthesis code MOOG, first described by Sneden (1973).

An initial step in the abundance analysis is the determination of the microturbulent velocities in our sample of stars. In order to find the microturbulent velocity, ξ, we chose a well-sampled species, in this case the Fe I lines, and demanded that both weak and strong lines yield consistent abundances. In Figure 5, we show a sample determination of ξ for HD 216219; here we plot [Fe/H] as a function of ξ for a sample of Fe I lines. Each line represents the Fe abundance as derived for an individual line as a function of the microturbulent velocity.

FIG. 4.—A comparison of C I and O I equivalent widths common to both this study and Luck & Bond (1982—LB82): the solid lines indicate perfect agreement. The top panel shows the C I equivalent widths while the O I lines are in the bottom panel. The overall agreement is good, although the LB82 C I equivalent widths tend to be slightly larger than from this work.

TABLE 2

EQUIVALENT WIDTHS

ELEMENT	λ (Å)	log *gf*	χ (eV)	EQUIVALENT WIDTHS (mÅ) HD 4395	HD 11377	HD 88446	HD 89948	HD 125079	HD 182274	HD 204613	HD 216219	HD 219116
C I	7111.48	−1.33	8.64	16	23	11	24	...	...	34	34	...
C I	7113.18	−0.96	8.64	26	33	20	29	34	33	39	35	30
C I	7115.19	−0.93	8.64	27	30	15	35	37	43	28	46	...
C I	7116.99	−1.10	8.64	18	28	24	28	26	28	26	39	...
C I	7119.67	−1.33	8.64	...	19	12	27	...	30	19	35	...
O I	7771.94	+0.33	9.11	62	118	96	82	58	109	88	97	51
O I	7774.17	+0.19	9.11	55	101	84	73	53	92	75	79	43
O I	7775.39	−0.03	9.11	42	78	64	62	42	73	65	63	35
Na I	6154.23	−1.57	2.10	35	26	16	21	48	21	27	27	41
Na I	6160.75	−1.27	2.10	46	42	27	33	71	30	43	40	57
Si I	6142.49	−1.51	5.62	35	35	18	27	44	24	35	29	32
Si I	6145.02	−1.50	5.61	37	33	21	27	41	24	32	29	34
Si I	6414.99	−1.15	5.87	48	41	30	40	54	36	47	43	43
Ca I	6161.30	−1.27	2.52	67	48	38	46	96	39	48	56	95
Ca I	6162.18	−0.15	1.90	193	167	144	172	218	154	174	167	194
Ca I	6166.44	−1.18	2.52	69	53	42	50	81	41	56	60	91
Ca I	6169.04	−0.86	2.52	91	76	66	66	111	62	77	74	109
Ca I	6169.56	−0.60	2.52	112	91	80	81	121	79	100	94	131
Ca I	6417.68	−0.55	4.44	14	9	8	8	24	10	9	12	19
Ca I	6439.08	−0.17	2.52	150	139	...	142	178	123	143	136	161
V I	6150.13	−1.47	0.30	17	9	...	4	31	...	8	9	32
Cr I	5345.81	−1.04	1.00	129	107	84	91	156	82	102	123	174
Cr I	5348.33	−1.30	1.00	95	73	68	...	...	61	78	83	129
Mn I	5117.94	−1.24	3.13	45	13	19	23	72	10	29	39	52
Mn I	5377.61	−0.06	3.84	35	31	16	33	77	20	31	37	53
Fe I	5109.66	−0.89	4.30	86	65	51	65	100	55	65	70	92
Fe I	5123.73	−3.24	1.01	146	99	96	108	202	84	115	142	...
Fe I	5126.12	−0.91	4.26	97	59	48	70	124	47	75	78	96
Fe I	5127.37	−3.44	0.91	118	86	79	81	151	70	97	106	153
Fe I	5133.70	−0.12	4.18	142	124	104	126	165	108	128	125	141
Fe I	5339.94	−0.67	3.26	138	109	103	117	152	101	108	118	149
Fe I	5361.63	−1.48	4.41	58	36	35	51	110	35	46	72	120
Fe I	5364.88	−0.26	4.44	101	107	86	104	128	97	100	109	129
Fe I	5365.41	−1.40	3.57	71	69	58	64	99	63	69	75	98
Fe I	5367.48	−0.01	4.41	104	114	96	115	126	101	109	111	126
Fe I	5369.97	−0.04	4.37	124	132	106	124	156	116	124	130	145
Fe I	5373.71	−0.97	4.47	45	53	39	45	76	39	47	50	68
Fe I	6136.62	−1.67	2.45	123	110	97	91	159	93	...	111	166
Fe I	6137.70	−1.57	2.59	130	106	90	100	159	90	106	112	162
Fe I	6151.62	−3.37	2.18	52	30	18	24	69	22	33	36	72
Fe I	6157.73	−1.33	4.07	65	51	36	48	89	43	49	67	99
Fe I	6159.39	−1.94	4.61	15	8	...	8	20	5	9	9	17
Fe I	6165.36	−1.62	4.14	43	32	23	25	55	21	31	32	51
Fe I	6173.34	−2.93	2.22	73	52	43	47	87	37	54	56	94
Fe I	6180.21	−2.73	2.73	59	38	30	36	79	27	40	43	88
Fe I	6408.03	−1.14	3.69	104	77	72	76	131	68	81	85	116
Fe I	6411.66	−1.17	3.65	121	98	83	98	132	86	97	99	124
Fe I	6419.96	−0.45	4.73	83	73	69	67	104	60	66	75	90
Fe I	6430.86	−2.24	2.18	112	96	86	90	141	81	93	107	155
Fe II	6149.25	−2.82	3.89	42	52	32	34	49	40	34	50	44
Fe II	6416.93	−2.82	3.89	44	54	43	36	52	40	35	51	49
Fe II	6432.68	−3.68	2.89	50	54	...	42	68	43	39	56	53
Co I	5342.71	+0.61	4.02	28	21	21	19	41	11	23	22	47
Co I	5352.05	+0.08	3.58	23	17	13	15	45	7	23	19	46
Ni I	5099.94	−0.20	3.68	100	74	62	73	118	61	86	90	107
Ni I	5115.40	−0.23	3.83	77	67	58	66	98	58	70	70	94
Ni I	6175.37	−0.54	4.09	51	41	30	32	56	28	38	43	52
Ni I	6176.82	−0.35	4.09	61	51	37	43	74	36	50	51	70
Ni I	6177.26	−3.45	1.83	19	...	...	...	31	...	10	10	17
Cu I	5105.45	−1.14	1.39	105	64	55	74	145	49	95	106	170
Y I	6435.05	−0.92	0.07	7	5	...	6	27	9	10	9	28
Y II	5119.12	−1.32	0.99	54	27	31	49	86	33	54	72	74
Zr I	6134.58	−1.03	0.00	8	...	...	6	16	...	...	...	18
Zr I	6143.23	−1.00	0.07	11	6	...	7	30	...	8	9	32
Zr II	5112.28	−0.74	1.66	39	18	25	38	...	27	41	56	63
Ba II	6141.75	+0.00	0.70	185	126	149	206	260	172	179	240	278
Nd II	5356.99	−0.24	1.26	12	7	11	9	43	11	12	31	63

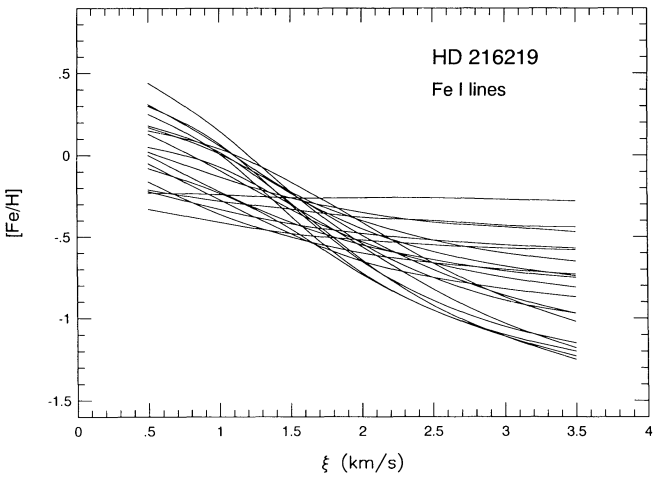

FIG. 5.—An illustration of the determination of the microturbulent velocity, ξ, for HD 216219. Each solid curve represents the Fe abundance, [Fe/H], as a function of ξ for a single Fe I line. The weaker Fe I lines have the least dependence of [Fe/H] with ξ, while the stronger lines change the most; the locus where the weak and strong lines cross is the best estimate of ξ. For HD 216219, $\xi = 1.6$ km s^{-1} with an uncertainty of about ± 0.3 km s^{-1}.

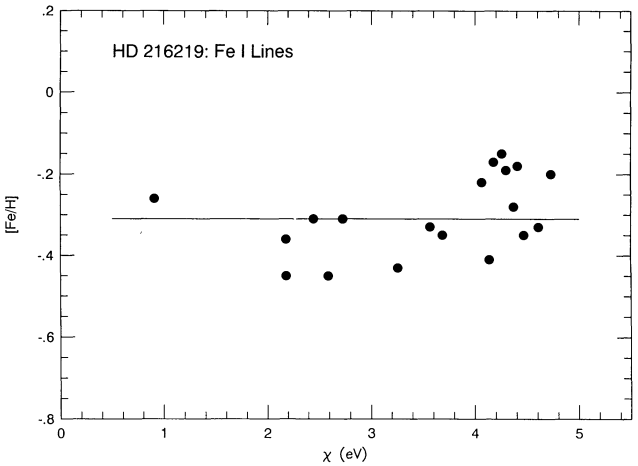

FIG. 6.—The Fe abundance ([Fe/H]) from the Fe I lines in HD 216219 as a function of lower level excitation potential, χ. The horizontal solid line is the mean of [Fe/H] = −0.29. There is no significant trend of [Fe/H] with χ, indicating a correct temperature distribution in the model atmosphere.

Where these lines cross, or more properly, where these lines most nearly converge, provides the best estimate for ξ. For HD 216219 we estimate a "best" microturbulent velocity of $\xi = 1.6$ km s^{-1}, with an uncertainty of about ± 0.3 km s^{-1}: this is typical for this sample of stars.

As a check of the values of $T_{\rm eff}$ and log g, Fe abundances as a function of excitation potential and Fe I and Fe II abundances were studied. Within the dispersion of abundances of our sample of Fe I lines (typically ± 0.15 dex), there is no trend in [Fe/H] with excitation potential: this we illustrate, again using HD 216219, in Figure 6 where we plot [Fe/H] versus the excitation potential (χ) for Fe I. The ionization equilibrium is also closely matched for our stellar parameters using Fe I and Fe II: for HD 216219 this difference is 0.05 dex ([Fe I/H] = -0.35 ± 0.10 and [Fe II/H] = -0.30 ± 0.06). This is typical for the stars in our sample with the greatest difference between Fe I and Fe II being 0.18 dex and the average difference being (Fe I–Fe II) = +0.06 dex: this suggests that our derived $T_{\rm eff}$/log g/ξ are not suffering from significant uncertainties.

Abundances we derived from the set of lines in Table 2, using the parameters as defined in Table 1, are listed in Table 3. We follow the convention of LB82 and list the C and O abundances on the scale of log ϵ(H) = 12, while for the other elements, we list their values in spectroscopic bracket notation: as these are derived from solar gf-values, these bracket abundances are determined relative to the Sun.

3. THE ABUNDANCES

We begin our discussion of the abundances by first comparing [Fe/H] derived here with those derived by LB82 or LB91; Fe has the most lines from which abundances are determined and a comparison between the two studies will tell us if there are significant systematic differences between us and LB82. In

TABLE 3

CH SUBGIANT ABUNDANCES

	STAR								
ELEMENT	HD 4395	HD 11377	HD 88446	HD 89948	HD 125079	HD 182274	HD 204613	HD 216219	HD 219116
log ϵ(C)	8.65±0.06	8.71±0.12	8.41±0.05	8.86±0.14	9.05±0.10	8.92±0.13	8.91±0.10	9.02±0.10	8.73
log ϵ(O)	8.65±0.02	9.06±0.07	8.86±0.05	8.77±0.05	8.73±0.03	9.03±0.06	8.95±0.03	8.93±0.09	8.48±0.06
[Fe/H]	−0.33±0.12	−0.05±0.08	−0.36±0.08	−0.27±0.11	−0.16±0.11	−0.18±0.11	−0.35±0.12	−0.32±0.10	−0.34±0.11
[Na/H]	−0.19	−0.06	−0.34	−0.20	+0.02	−0.23	−0.20	−0.24	−0.18
[Si/H]	−0.08	+0.05	−0.27	−0.11	0.00	−0.16	−0.09	−0.20	−0.18
[Ca/H]	−0.03±0.06	−0.05±0.05	−0.30±0.11	−0.12±0.03	−0.01±0.03	−0.26±0.06	−0.16±0.09	−0.18±0.05	−0.13
[V/H]	−0.20	+0.109	...	−0.34	−0.06	...	−0.34	−0.32	−0.14
[Cr/H]	−0.17	−0.07	−0.32	−0.10	+0.09	−0.31	−0.30	−0.48	−0.30
[Mn/H]	−0.10	−0.19	−0.29	−0.09	+0.06	−0.38	−0.20	−0.31	−0.08
[Co/H]	−0.29	−0.11	−0.17	−0.18	−0.04	−0.43	−0.20	−0.33	−0.05
[Ni/H]	−0.12±0.12	−0.04±0.02	−0.28±0.04	−0.12±0.14	−0.11±0.08	−0.26±0.05	−0.24±0.13	−0.30±0.10	−0.28
[Cu/H]	−0.18	−0.40	−0.53	−0.19	...	−0.60	−0.14	−0.16	+0.02
[Y/H]	+0.40	+0.24	+0.48	+0.84	+1.06	+0.59	+0.72	+0.80	+0.64
[Zr/H]	+0.31	+0.38	+0.51	+0.62	+0.68	+0.61	+0.50	+0.55	+0.47
[Ba/H]	+0.23	−0.02	+0.28	+0.56	+0.59	+0.41	+0.21	+0.57	+0.56
[Nd/H]	+0.09	+0.21	+0.50	+0.33	+0.69	+0.62	+0.27	+0.65	+1.09 −0.37

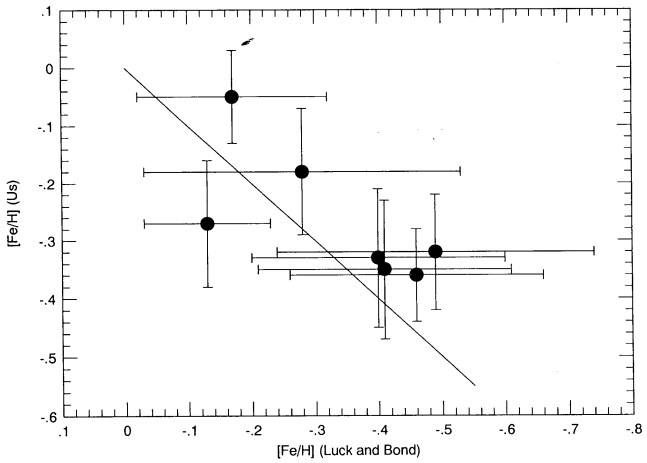

FIG. 7.—A comparison of [Fe/H] as derived by us compared to Luck & Bond (1982—LB82) for CH subgiants in common. The agreement is close, although our values of [Fe/H] tend to be ≈0.05–0.10 dex larger than LB82. The solid line illustrates perfect agreement.

Figure 7 we plot our [Fe/H]'s versus those from LB82 (with one star from LB91) for stars we have in common: the solid line represents a perfect agreement between the two determinations. It is clear from Figure 7 that the agreement between our Fe abundances and LB's is good, with differences less than about 0.1 dex, although we derive a systematically larger [Fe/H] by about 0.1 dex: the mean and standard deviation of $\bar{\Delta}$(us − LB) = +0.07 ± 0.10. The results suggest that our abundances can be safely compared to LB82. Krishnaswamy & Sneden (1985) have also determined [Fe/H] for two stars in our sample (HD 4395 and HD 216219) and the comparisons are also good, with differences between our value minus their's of −0.01 dex and +0.22 dex, respectively, for each star.

One goal of our study here was to investigate the rather large C/O ratios obtained by LB82 for many of the CH subgiants and, as we used the same lines to determine the C and O abundances, a direct comparison of these abundances is in order. LB82 determined C and O abundances for five stars that we have in common, and we show the comparisons between their abundances and ours in Figure 8: here in the top panel we plot our C abundances versus their C abundances, while in the bottom panel we compare the O abundances. In studying the C abundances from LB82, we noted that in four stars one line of C I from each star yielded C abundances which were far from the means of the other four lines, so in these stars we rejected this discrepant line and rederived C abundances using the LB82 stellar parameters. The stars and C I lines were the 7111.48 Å line in HD 4395 and HD 182274, the 7116.99 Å line in HD 88446, and the 7119.67 Å line in HD 89948. In all cases, the discrepant line was too strong and we note that telluric H_2O contaminates this region; thus, it is possible that imperfect division of the telluric H_2O may lead to a discrepant C I line. The resulting comparison of the abundances reveals excellent agreement with LB82, as would be expected from the overall good agreement in the C I equivalent width shown in Figure 4. For oxygen, shown in the bottom panel of Figure 8, the agreement between our abundances and LB82 is very good for four out of five stars, with LB82 deriving a larger O abundance for HD 216219. We note only that the LB82 equivalent widths are larger than our values and we have no obvious explanations for this. The good agreement between our abundances and those of LB82 means that we also find rather large C/O ratios for some of the CH subgiants, as can be seen by an inspection of Table 3: C/O ratios range from 0.4 to 2.1.

Recently, Tomkin et al. (1992) have presented an extensive analysis of these same C I and O I lines in metal-poor dwarfs, and we can discuss some aspects of our results in light of these recent results: the CH subgiants overlap in $T_{\rm eff}$ and log g the dwarfs studied by Tomkin et al., although their sample of stars covered considerably lower metallicities from [Fe/H] = −0.8 to −2.6. The first issue is that of non–LTE effects influencing the formation of these high-excitation permitted lines. Tomkin et al. (1992) carried out non–LTE calculations which included realistic UV radiation fields based upon the line opacities as described in Kurucz (1979) and including neutral H-collisions as suggested by Steenbock & Holweger (1984). Their straightforward results indicate that non–LTE processes change the derived LTE abundances by only a small amount: ∼0.05 dex, or less. These results agree with sample non–LTE calculations for C I and O I done for our model for HD 216219 kindly carried out by M. Lemke (1991).

Despite the inclusion of a non–LTE analysis, Tomkin et al. (1992) still find, for their sample of metal-poor dwarfs, increasing values of [C/Fe] and [O/Fe] with decreasing $T_{\rm eff}$, which they argue must originate with still unknown systematic effects. They speculate that the improper treatment of convec-

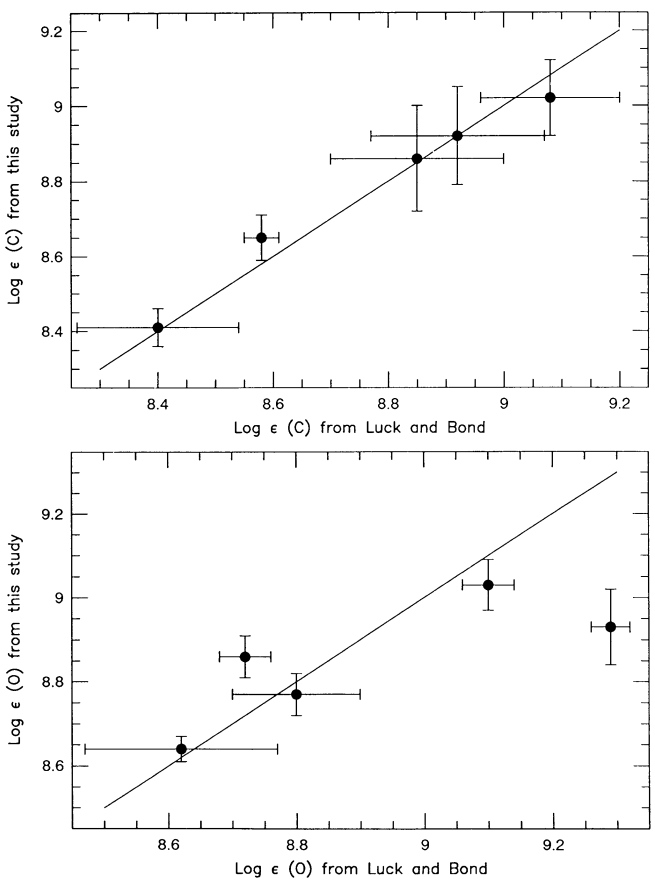

FIG. 8.—A comparison of the C and O abundances for stars in common to this study and that of LB82: the top panel shows the C abundances while the bottom shows the O abundances and the solid lines show perfect agreement. The agreement of the abundances is excellent, with the exception of O in one star in which LB82's O I equivalent widths are larger than ours.

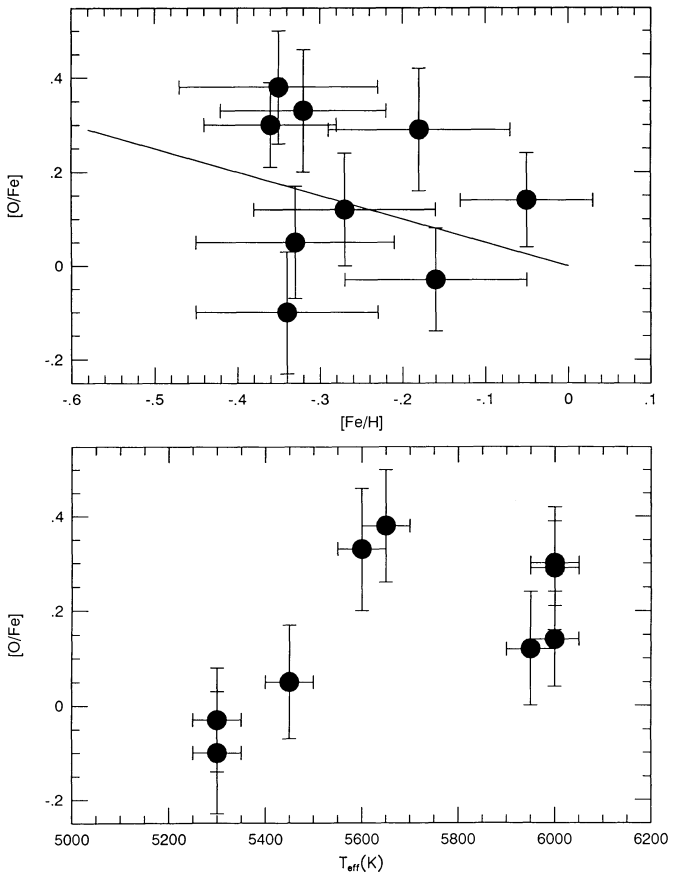

FIG. 9.—An examination of the oxygen abundances; in the top panel, [O/Fe] is plotted vs. [Fe/H]. The solid line represents the general trend observed for [O/Fe] as a function of [Fe/H]: the derived [O/Fe] abundances for the CH subgiants scatter about the general relation. The bottom panel illustrates [O/Fe] vs. T_{eff}. Our temperature range and sample size is limited, but no significant trend is found in [O/Fe] as a function of T_{eff}.

tion and granulation in these metal-poor dwarfs might be responsible for the temperature effects in the C I and O I lines. We investigate possible systematic effects in our O abundances by examining [O/Fe] as functions of [Fe/H] and T_{eff}, as shown in Figure 9. As the CH subgiants have had their ^{12}C abundances altered by triple-α burning, but quite probably not their ^{16}O abundances, we restrict our comparison to the O abundances. In the top panel we show how our derived [O/Fe] varies with metallicity, [Fe/H]; the solid line represents the general trend found for the interval [Fe/H] = 0.0 to −0.1 of [O/Fe] = $-0.5 \times$ [Fe/H], as reviewed, for example, in Wheeler, Sneden, & Truran (1989). Clearly, our [O/Fe] values scatter about the mean trend observed for dwarf stars and no obvious trends away from the mean are seen. In the lower panel is plotted [O/Fe] versus T_{eff}; here there may be a slight trend with [O/Fe] decreasing with decreasing T_{eff}, however, our sample is small and the mean of [O/Fe] = +0.16 is an approximation to the spread of points. There are no apparent significant trends in our O abundances and we note that (1) our sample of subgiants have significantly larger metallicities than the Tomkin et al. (1992) sample, and (2) we used scaled-solar model atmospheres, while their analysis used MARCS models. These differences, coupled with our small sample, may mask small systematic (~0.1–0.2 dex) trends in our C and O abundances, if they exist. Tomkin et al. (1992) did find, however, that there was no trend in the C/O ratios, as derived from both LTE and non–LTE analyses of the C I and O I lines, as functions of T_{eff}. As the C/O ratio is what we are really interested in, these results strengthen our result that some of the CH subgiants exhibit quite large C/O ratios.

In Figure 10 we show our derived C/O ratios compared to those from LB82, for stars in common, in the top panel and a comparison with Sneden (1983) in the bottom panel: the solid lines indicate perfect agreement. Our C/O ratios are in excellent agreement with those from LB82 except for HD 216219 where our respective O I equivalent widths do not agree (LB82's are larger, thus their C/O ratio is lower). For the three stars in common with Sneden (1983), we are in excellent agreement for one star and our C/O ratios are 40%–50% larger for the other two. Sneden used C_2 and the [O I] 6300 Å line to determine C and O abundances; thus, some differences may be inherent in our analyses—however, as is apparent from Figure 10, the uncertainties in the C/O ratios are rather large, and the differences are not much greater than the estimated uncertainties.

We now discuss the C, O, and *s*-process abundances of the CH subgiants and compare them to the other two classes of low-luminosity stars with carbon and *s*-process enhancements: the CH giants and the barium stars.

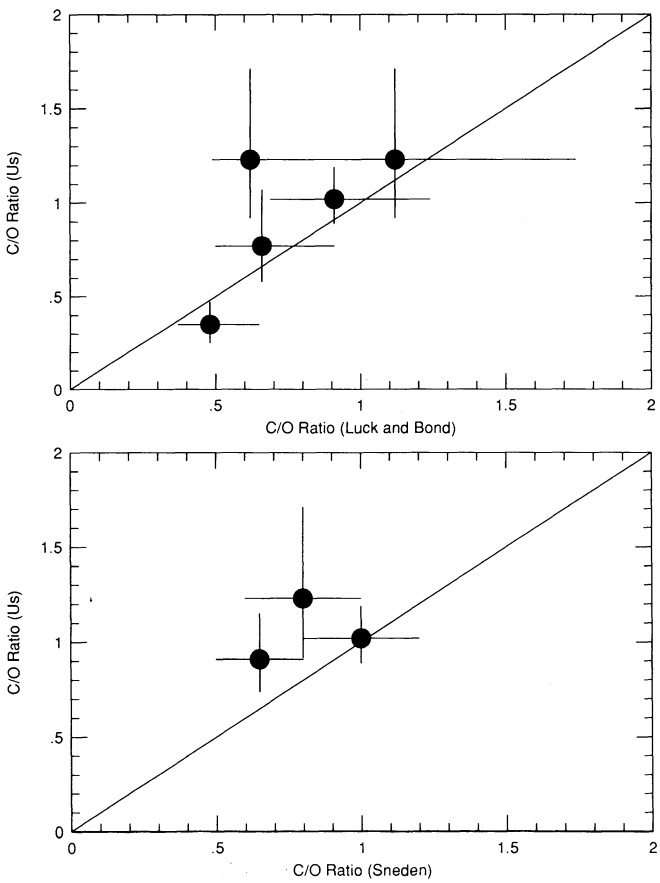

FIG. 10.—A comparison of the C/O ratios derived here with those of Luck & Bond (1982) and Sneden (1983). Errors are estimated from the quadrature sums of the uncertainties, in the respective C and O abundances. Except for perhaps two discrepant stars, the overall agreement, within the uncertainties, is good.

4. DISCUSSION

We have a set of C, O, and a limited number of *s*-process abundances, along with metallicities, for nine CH subgiants; we discuss these abundances within the broader context of the barium and CH giant stars. Do the abundances of these stars point to their having a common origin? All three groups, the barium stars and the CH giants and subgiants, are spectroscopic binaries with probable white-dwarf companions (McClure & Woodsworth 1990) and, thus, the ^{12}C and *s*-process overabundances have been hypothesized to result from mass transfer from the former AGB star, now a white dwarf, in the system.

Within the last decade, a number of abundance analyses have been carried out for the various "low-luminosity" (less than AGB luminosities) peculiar-abundance stars discussed here and we will now compare these abundances; for the barium stars, we take the results from Smith, Sneden, & Pilachowski (1980), Sneden, Lambert, & Pilachowski (1981), Kovacs (1983, 1985), Tomkin and Lambert (1983, 1986), Smith (1984) and Barbuy et al. (1992): for the CH giants we use the recent results from Vanture (1982a, b): for the CH subgiants we use the results here, which are very similar to Luck & Bond (1982), as well as some results from Luck & Bond (1991), although this recent paper does not include C or O and concentrates on the *s*-process elements.

In Figure 11, we combine the C/O ratios (with $C = {}^{12}C + {}^{13}C$, where the $^{12}C/^{13}C$ ratio has been determined) as a function of [Fe/H] for the various samples: the barium stars are the open symbols, with the CH stars shown as filled symbols (circles are subgiants and triangles are giants). Vanture's results for the low-metallicity CH giants stand out in this figure and provide significant weight to a trend of increasing C/O ratio with decreasing [Fe/H]. Although not so apparent when plotted at this scale, the CH subgiants have slightly larger C/O ratios than the barium giants; however, these two groups largely overlap in both C/O and [Fe/H], along with the more metal-rich CH giants. Since the discovery by Blanco, Blanco, & McCarthy (1978) that the ratio of the number of carbon star to the late M stars in the Small and Large Magellanic Clouds (SMC and LMC) and the Galactic bulge increases with decreasing metallicity, it has been suggested that the low initial O abundance at low [Fe/H] requires less carbon to be added to a star's atmosphere to produce $C/O > 1$. Figure 11 supports this conclusion and even supports the picture that the amount of ^{12}C added to a carbon star atmosphere is nearly independent of metallicity. The solid line in Figure 11 represents the simple scheme of adding a constant mass fraction of ^{12}C to a reservoir of material containing decreasing amounts of ^{12}C and ^{16}O: we decreased the ^{12}C and ^{16}O abundances using the prescriptions that $[^{12}C/Fe] \propto [Fe/H]$ while $[^{16}O/Fe] \propto -0.5[Fe/H]$ down to $[Fe/H] = -1.0$, after which $[^{16}O/Fe] = +0.5$ (Tomkin et al. 1992). We fix this relation at the metal-rich end using the barium stars and CH subgiants by setting $C/O = 0.85$ at $[Fe/H] = 0.0$; the resulting curve, based upon this very simple model, does a reasonable job of connecting Vanture's results at low [Fe/H] with the number of studies done at the higher metallicity end.

A comparison of the C/O ratios and *s*-process enhancements for the CH giants and subgiants is shown in Figure 12: here we plot ['*s*'/Fe] where '*s*' represents the average abundances of the four elements Y, Zr, Ba, and Nd, versus log (C/O) and we show the standard deviations of the mean of the various lines used in our results as the error bars. Except for HD 88446 among the CH subgiants, which has a larger ['*s*'/Fe] at rather low log (C/O), the CH subgiants represent a tight, direct correlation of increasing ['*s*'/Fe] with log (C/O) as shown by the straight line. When continued on to the extreme C/O ratios observed in Vanture's (1992a, b) metal-poor CH giants, the

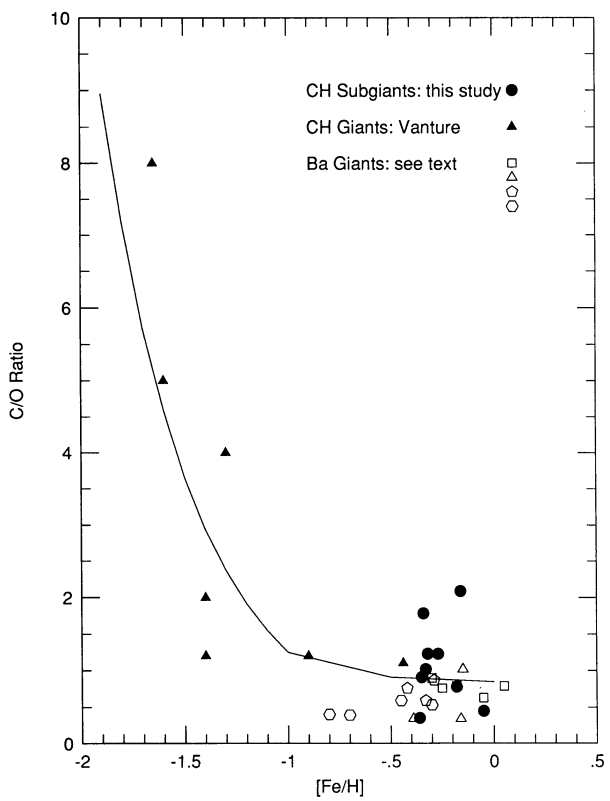

FIG. 11.—A comparison of C/O ratios as a function of [Fe/H] for barium giants (*open symbols*), CH giants (*filled triangles*), and CH subgiants (*filled circles*). The solid line is the resultant C/O ratio from the simple scheme of adding a constant mass fraction of ^{12}C to an envelope of decreasing C and O initial abundances with the curve fixed at $[Fe/H] = 0.0$ with $C/O = 0.85$.

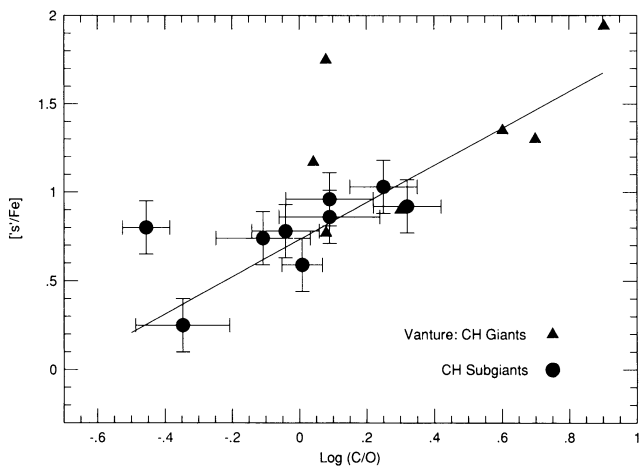

FIG. 12.—A comparison of the mean *s*-process overabundances (['*s*'/Fe]) and the C/O ratios in the CH subgiants studied here and the CH giants from Vanture (1992a, b). There is a general trend of ['*s*'/Fe] increasing with C/O for both the CH subgiants and giants.

straight line derived from the CH subgiants continues to be a reasonable approximation to these stars, indicating that, in many of these stars, the total amount of *s*-process elements mixed, or transferred, onto these stars scales directly with the amount of ^{12}C. As the amount of ^{12}C produced is roughly independent of metallicity (see Fig. 11), the amount of *s*-process material can also be tolerably fitted as being independent of metallicity. This increase in [‘*s*’/Fe] with decreasing [Fe/H] was noted first, in the form of [Ba/Fe], by Rocca-Volmerange & Audouze (1979) and later discussed by Kovacs (1985). A more striking extension of this effect of an increase in [‘*s*’/Fe] at low metallicities is a comparison of the heavier *s*-process elements (such as Ba, La, or Nd) to the lighter *s*-process abundances (such as Sr, Y, or Zr) as a function of [Fe/H]; the ratio of “heavy-*s*” to “light-*s*,” [*hs*/*ls*], is a sensitive function of the total neutron irradiation, the neutron exposure, and Luck & Bond (1991) and Vanture (1992b) show this to increase with decreasing [Fe/H]. Clayton (1988) has shown that such an increase in the neutron exposure with decreasing [Fe/H] should occur if the neutron source for the *s*-process is $^{13}C(\alpha, n)^{16}O$, with the ^{13}C being the result of the mixing of protons into the regions that have experienced ^{4}He-burning followed by $^{12}C(p, \gamma)^{13}C$. The increase in the strength of the *s*-process with decreasing metallicity comes from the combination of the ^{13}C neutron source being independent of metallicity while the total amount of *s*-process neutron poisons decreases as approximately $1/Z$. The combined studies of the barium stars plus CH giants and subgiants provide support for the *s*-process being driven primarily by $^{13}C(\alpha, n)^{16}O$.

In Figure 13, we show a comparison of the *s*-process overabundances, [‘*s*’/Fe], with the C/O ratios in the barium stars and the CH subgiants: the extremely metal-poor CH giants from Vanture (1992a, b) fall well off this figure at large C/O ratios. We include also the N-type carbon stars in which *s*-process abundances were determined by Utsumi (1985) and the C/O ratios are taken from Lambert et al. (1986). The position of the C/O ratios for G and K giants from Lambert & Ries (1981) is also shown (assuming [‘*s*’/Fe] $\approx$ 0.0), along with the solar position. Clearly, the C/O ratios of the CH subgiants fall at systematically larger C/O ratios than the barium stars; however, as the CH subgiants lie on, or near, the main sequence, their convective envelopes will deepen substantially as they evolve onto the red giant branch. If the ^{12}C- and *s*-process-rich material now on the surface is mixed with normal abundance matter, the C/O ratios and [‘*s*’/Fe] will decrease. A 50–50 mixture of such material will move CH subgiants in Figure 13 such that the CH subgiant distribution will closely match the barium star distribution. These results for the C/O ratios and *s*-process abundances indicate that the barium giants could evolve from CH subgiant progenitors near the main sequence.

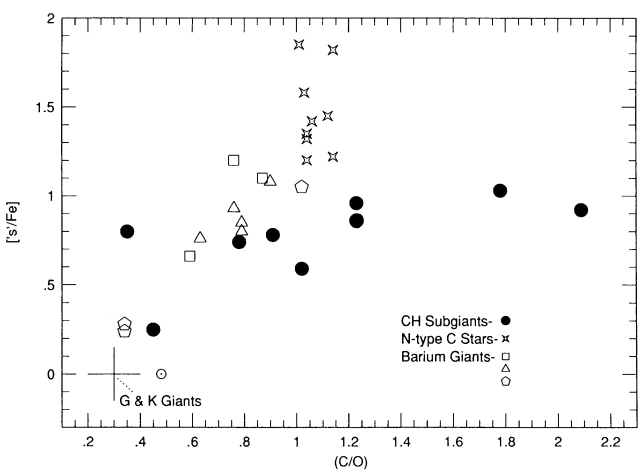

FIG. 13.—Mean *s*-process overabundances ([‘*s*’/Fe]) and C/O ratios in the CH subgiants (*filled circles*), barium giants and N-type carbon stars. The CH subgiants tend to have larger C/O ratios than the barium giants; however, the deepening convective envelope which will form in the CH subgiants as they evolve up the giant branch will lower their C/O ratios and [‘*s*’/Fe] and probably shift them onto the barium giant sequence.

Another set of observations that is consistent with the hypothesis that CH subgiants evolve into barium giants are the measurements of $^{12}C/^{13}C$ ratios in these two types of stars. Sneden (1983) estimates that the carbon isotope ratios are typically $^{12}C/^{13}C \gtrsim 40$ or $^{12}C/^{13}C \sim 20$–60 in five CH subgiants. Measurements in the barium giants have been done by Tomkin & Lambert (1979); Sneden et al. (1981); Smith (1984); or Barbuy et al. (1992), who find $^{12}C/^{13}C$ to be almost completely in the range 7–20 for 13 barium giants. The rather large $^{12}C/^{13}C$ ratios estimated for the CH subgiants are consistent with the picture of these stars accreting S-star or N-type carbon star material, with typical $^{12}C/^{13}C$ ratios of 20–100 (Lambert et al. 1986; Smith and Lambert 1990), as main-sequence stars. The lower $^{12}C/^{13}C$ ratios of the barium giants is then the result of the mixing of CN-processed material during the first ascent of the giant branch.

One inconsistency to the hypothesis that CH subgiants evolve into barium giants was provided by Li abundances in these two groups of stars. This inconsistency was emphasized by Smith & Lambert (1986), who determined upper limits to the Li abundance in a sample of CH subgiants and compared them to the published Li abundances in the barium giants by Pinsonneault, Sneden, & Smith (1984); more recent estimates of the Li abundances in barium giants by Barbuy et al. (1992) agree with the Pinsonneault et al. determinations. The problem arose because the observed upper limits to Li in CH subgiants overlapped the range of the reported Li abundances in the barium giants. When the expected convective dilution of Li (due to evolution up the red giant branch) was applied to the upper limits of the CH subgiant abundances (a factor of 40), the resultant predicted Li abundances for the barium giants was about a factor of 10 less than the published abundances. This discrepancy led Smith & Lambert (1986) to propose that the CH subgiants and barium giants were on separate evolutionary paths (although both were the result of mass transfer), with the mass transfer occurring at different times in the evolution of the mass-accreting star. Recent work by Lambert, Smith, & Heath (1993) has now removed this discrepancy in the Li abundances; they find that an unidentified *s*-process line (which correlates with the Ce II line strengths) is a major contributor in the barium giants to the absorption feature attributed in previous studies to a blend of CN lines and the Li I resonance doublet. Lambert et al. (1993) find good fits to the observed spectra of barium giants without significant contributions from Li I: the estimated Li abundances in the barium giants are now in agreement with the upper limits set for the CH subgiants coupled with the expected convective dilution of Li as the CH subgiants evolve into giants.

5. SUMMARY

The fact that the CH subgiants exhibit similar abundance patterns as observed in the more luminous barium giants (^{12}C and *s*-process overabundances), as well as the fact that both

types of star are found in binary systems with white-dwarf companions, lends support to the idea that CH subgiants evolve into the barium giants, as suggested by Luck & Bond (1991). The C/O ratios and *s*-process abundances derived here support this picture, provided that the material now observed in the atmospheres of the CH subgiants is mixed with enough material of normal *s*-process composition ([‘*s*’/Fe] = 0.0) and normal ^{12}C (or slightly depleted in ^{12}C due to the mixing of material exposed to the CN cycle) composition to lower the C/O ratio by a factor of 2 or 3 as the CH subgiant evolves up the giant branch. As the convective envelope of a red giant is quite massive ($\sim 0.5\ M_{\odot}$), the fact that CH subgiants retain their abundance peculiarities as they ascend the giant branch requires that substantial amounts of mass be accreted from the former AGB star onto the CH subgiant.

When combined with the recent work by Vanture (1992a, b) on the metal-poor CH giants, a unified picture emerges for all of the low-luminosity, *s*-process, and ^{12}C-rich stars as having accreted substantial amounts of mass from a thermally pulsing AGB star in which the *s*-process is driven by the $^{13}C(\alpha, n)^{16}O$ neutron source.

We thank Dr. Andrew Vanture for helpful discussions. This research has been supported in part by the Robert A. Welch Foundation of Houston, Texas, and the National Science Foundation (grant AST 91-15090).

REFERENCES

Anders, E., & Grevesse, N. 1989, Geochim. Cosmochim. Acta, 53, 197
Barbuy, B., Jorissen, A., Rossi, S. C. F., & Arnould, M. 1992, A&A, 262, 216
Blanco, V. M., Blanco, B. M., & McCarthy, M. R. 1978, Nature, 271, 638
Bond, H. E. 1974, ApJ, 204, 810
Clayton, D. D. 1988, MNRAS, 234, 1
Debouille, L., Neven, L., & Roland, G. 1973, Photometric Atlas of the Solar Spectrum from λ3000 to λ10000 Å (Liège: Institut d'Astrophysique)
Grevesse, N., Lambert, D. L., Sauval, A. J., van Dishoeck, E. F., Farmer, C. B., Norton, R. H. 1991, A&A, 242, 488
Harris, H. C., & McClure, R. D. 1983, ApJ, 265, L77
Hoffleit, D., & Jashek, C. 1982, The Bright Star Catalogue (New Haven: Yale Univ. Observatory)
Holweger, H., & Müller, E. A. 1974, Sol. Phys., 39, 19
Kovacs, N. 1983, A&A, 120, 21
———. 1985, A&A, 150, 232
Krishnaswamy, K., & Sneden, C. 1985, PASP, 97, 407
Kurucz, R. L. 1979, ApJS, 40, 1
Lambert, D. L. 1985, in Cool Stars with Excesses of Heavy Elements, ed. M. Jaschek & P. C. Keenan (Dordrecht: Reidel), 191
Lambert, D. L., Gustafsson, B., Eriksson, K., & Hinkle, K. H. 1986, ApJS, 62, 373
Lambert, D. L., & Ries, L. M. 1981, ApJ, 248, 228
Lambert, D. L., Smith, V. V., & Heath, J. 1993, PASP, 105, 568
Lemke, M. 1991, private communication
Luck, R. E., & Bond, H. E. 1982, ApJ, 259, 792
———. 1991, ApJS, 77, 515
McClure, R. D. 1983, ApJ, 268, 264
———. 1984, ApJ, 280, L31
McClure, R. D. 1989, in Evolution of Peculiar Red Giant Stars, ed. H. R. Johnson & B. Zuckerman (Cambridge: Cambridge Univ. Press), 101
McClure, R. D., Fletcher, J. M., & Nemec, J. M. 1980, ApJ, 238, L35
McClure, R. D., & Woodsworth, A. W. 1990, ApJ, 352, 709
Pinsonneault, M. H., Sneden, C., & Smith, V. V. 1984, PASP, 96, 239
Rocca-Volmerange, B., & Audouze, J. 1979, A&A, 75, 371
Smith, V. V. 1984, A&A, 132, 326
Smith, V. V., & Lambert, D. L. 1986, ApJ, 311, 843
———. 1990, ApJS, 72, 387
Smith, V. V., Sneden, C., & Pilachowski, C. A. 1980, PASP, 92, 809
Sneden, C. 1973, Ph.D. thesis, Univ. Texas at Austin
———. 1983, PASP, 95, 745
Sneden, C., & Bond, H. E. 1976, ApJ, 204, 810
Sneden, C., Lambert, D. L., & Pilachowski, C. A. 1981, ApJ, 247, 1052
Steenbock, W., & Holweger, H. 1984, A&A, 130, 319
Tomkin, J., & Lambert, D. L. 1979, ApJ, 227, 209
———. 1983, ApJ, 273, 722
———. 1986, ApJ, 311, 819
Tomkin, J., Lemke, M., Lambert, D. L., & Sneden, C. 1992, AJ, 104, 1568
Utsumi, K. 1985, in Cool Stars with Excesses of Heavy Elements, ed. M. Jaschek & P. C. Keenan (Dordrecht: Reidel), 243
Vanture, A. D. 1992a, AJ, 104, 1986
———. 1992b, AJ, 104, 1997
Wheeler, J. C., Sneden, C., & Truran, J. W. 1989, ARA&A, 27, 279
Wiese, W. L., Glennon, B. M., & Smith, M. W. 1966, Atomic Transition Probabilities, NSRDS-NBS-4 (Washington, DC: USGPO)